

# Potential Catalyst Deactivation Reaction in Homogeneous Ziegler–Natta Polymerization of Olefins: Formation of an Allyl Intermediate

Peter M. Margl, Tom K. Woo, and Tom Ziegler\*

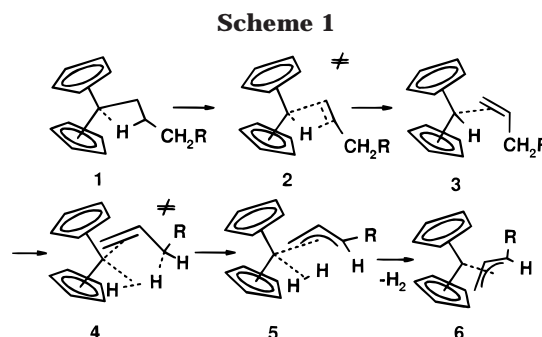
Department of Chemistry, The University of Calgary, 2500 University Drive NW, Calgary, Alberta, Canada

Received May 26, 1998

We investigate the possibility of premature deactivation of  $d^0$  transition metal Ziegler–Natta metallocene catalysts  $Cp'_2MR^+$  ( $Cp'$  = any cyclopentadienyl derivative) used in homogeneous olefin polymerization. Density functional calculations show that  $\beta$ -hydride elimination from the  $\beta$ -agostic precursor likely leads to formation of an allyl dihydrogen complex. This complex is prone to eject the dihydrogen ligand and form a “torpid”  $Cp'_2M(allyl)^+$  complex that can be slow to restart chain propagation, depending on the steric hindrance imposed on the metal by the  $Cp'$  moiety. Our theoretical observations are in line with previous experimental evidence for such a reaction.

## Introduction

Group 4 metallocenes are valuable catalysts for the production of polyolefins with a wide range of specifications.<sup>1</sup> Under industrial process conditions, however, they are known to suffer from slow deactivation. The rate of deactivation depends on a variety of issues, most of which are simply process-related and may be due to feed impurity and decomposition at high temperature, but they are also known to depend on the structure of the catalyst.<sup>2</sup> We have recently found theoretical evidence for the formation of a very stable allyl intermediate that arises from occasional  $\beta$ -hydride eliminations from the agostic precursor.<sup>3</sup> This allyl intermediate is supposed to be relatively inert (“torpid”) with respect to further insertions of monomer. Such allyl intermediates have been detected or postulated in previous experimental work by Richardson et al.<sup>4</sup> and a group from Union Carbide.<sup>5</sup> The reaction path for the formation of the allyl from a polyethylene chain dangling from an active site is shown in Scheme 1 for the case of a simple bis-Cp system. The initiator for allyl formation is a  $\beta$ -elimination process (1–3), whereby a hydrogen atom of the growing chain is abstracted by the metal to form a metal hydride olefin species. Subsequently, one of the  $\gamma$ -hydrogen atoms of the vinyl-terminated chain is brought into the vicinity of the hydride by a low-barrier rotation of the chain. The  $\gamma$ -hydrogen is abstracted to form a dihydrogen allyl species (4, 5). The dihydrogen ligand may subsequently be ejected, giving rise to a “naked” allyl species (6). Our previous results, based on density functional molecular dynamics,<sup>3</sup> have shown that this process is quite facile



for the Ti-“constrained-geometry” catalyst  $(SiH_2)Cp-(NH)R^+$  and that in fact almost every  $\beta$ -elimination that occurs should liberate one dihydrogen molecule. There is substantial evidence that dihydrogen production occurs during catalytic polyolefin production, although literature on the topic is scarce.<sup>5</sup> Likewise, as pointed out by Karol et al.,<sup>5</sup> liberation of dihydrogen stemming from this mechanism would inevitably leave traces (such as internal unsaturation) in the resultant polymer if polymerization were to continue from the allyl species (6). Furthermore, if the allyl species 6 were sufficiently inert with respect to reinsertion of an olefin monomer, the chain growth mechanism would be impaired to varying degrees, depending on the kinetic stability of the allyl. An allyl species that is inert enough to accumulate over time would eventually lead to deactivation of the catalyst. Of course, catalyst activity would also be impaired if one of the reaction products of the allyl complex with monomer were inert. Recently, Resconi<sup>2</sup> has managed to explain a number of experimental observations pertaining to propylene polymerization in a consistent manner by this mechanism. We will in the following use theoretical calculations to answer the following questions that pertain to the much simpler case of ethylene polymerization: (a) how likely is an occurrence of the allyl–dihydrogen mechanism for a typical metallocene-type catalyst? (b) Can the allyl–

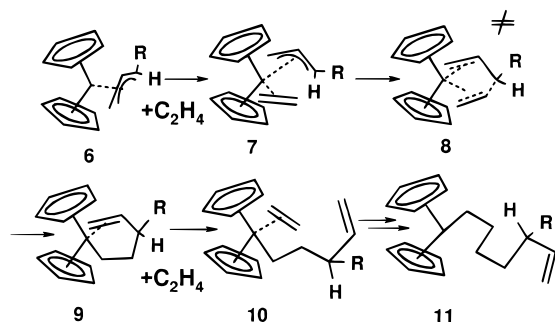
(1) Brintzinger, H. H.; Fischer, D.; Mülhaupt, R.; Rieger, B.; Waymouth, R. M. *Angew. Chem., Int. Ed. Engl.* **1995**, *34*, 1143–1170.  
(2) Resconi, L. Private communication, 1998.

(3) Margl, P. M.; Woo, T. K.; Blöchl, P. E.; Ziegler, T. *J. Am. Chem. Soc.* **1998**, *120*, 2174–2175.

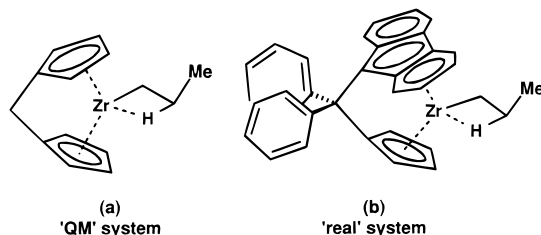
(4) Richardson, D. E.; Alameddini, G. A.; Ryan, M. F.; Hayes, T.; Eyler, J. R.; Siedle, A. R. *J. Am. Chem. Soc.* **1996**, *118*, 11244.

(5) Karol, F.; Kao, S.-C.; Wasserman, E. P.; Brady, R. C. *New J. Chem.* **1997**, *21*, 797.

Scheme 2



Scheme 3



dihydrogen mechanism indeed lead to eventual deactivation of the catalyst?

As a sample catalyst, we here employ the DPZ catalyst [diphenylmethylene(cyclopentadienyl-9-fluorenyl)zirconium] shown in Scheme 3b. We chose this particular system, as it is one for which dihydrogen evolution is well documented in the literature by Karol et al.<sup>5</sup> We utilize density functional theory (DFT)<sup>6</sup> as embodied in the ADF program<sup>7</sup> to simulate the bond breaking and making processes at the Zr center. Since the fluorenyl ligands as well as the phenyl substituents on the ansa-bridge are supposed to interact with the catalytic site only through steric pressure, they are included in our calculations through a molecular mechanics (MM) force field. The feasibility of this combined quantum-mechanical/molecular-mechanical (QM/MM) approach has been successfully demonstrated for ethylene polymerization catalysts.<sup>8</sup> Details of our calculations follow in the next section.

### Computational Details

**Density Functional Theory.** All reported DFT calculations were performed by means of the Amsterdam Density Functional (ADF) program system.<sup>9</sup> The electronic configurations of the molecular systems were described by a triple- $\zeta$  basis set<sup>10,11</sup> on the metal center valence, 5s, and 5p orbitals. A double- $\zeta$  STO basis set was used for carbon (2s, 2p) and hydrogen (1s), augmented with a single 3d polarization function except for hydrogen, where a 2p function was used. The inner shells on the metal (including 3d) and the carbon 1s orbitals were treated within the frozen-core approximation. A set of auxiliary<sup>12</sup> s, p, d, f, and g STO functions, centered on

all nuclei, was used to fit the molecular density and present Coulomb and exchange potentials accurately in each SCF cycle. Energy differences were calculated by augmenting the local exchange–correlation potential by Vosko et al.<sup>13</sup> with Becke's nonlocal exchange corrections<sup>14</sup> and Perdew's nonlocal correlation corrections<sup>15,16</sup> (BP86) in a self-consistent manner. Geometries were optimized including nonlocal corrections. First-order scalar relativistic corrections<sup>17,18</sup> were added to the total energy. This has been shown previously to be accurate for 4d metals such as Zr.<sup>19</sup> In view of the fact that all systems investigated in this work show a large HOMO–LUMO gap, a spin-restricted formalism was used for all calculations.

**QM/MM Coupling.** The ADF program system was modified to include the AMBER95<sup>20</sup> molecular mechanics force field in such a way that the QM (i.e., DFT) part and MM parts are coupled self-consistently, according to the method prescribed by Maseras and Morokuma.<sup>21</sup> In the combined QM/MM calculations, the QM part consisted of the “generic” complex [Scheme 3a] in which the fluorenyl benzene rings are removed from the central Cp ring, and the resulting Cp unsaturation is “capped” with hydrogen atoms. Hydrogens replace the phenyl substituents on the ansa-bridge in the generic system. Both phenyl substituents and benzo rings are treated by the MM method. The QM and MM parts were linked by the “capping” hydrogen atoms and coupled by van der Waals interactions. The geometry optimization on the whole system was carried out with coupling between QM and MM atoms. In the optimization of the MM part the C–C bonds crossing the QM–MM border were constrained to be 0.31 Å longer than the optimized C–H distance.

The AMBER95 force field<sup>20</sup> was augmented to describe the molecular mechanics potential. (All force field parameters are provided as supporting material.) Employing the AMBER atom type labels as described in ref 20, the carbon atoms on the auxiliary ligands were assigned the atom type “CA”, with the exception of the ansa-bridge carbon, which was assigned with atom type “CT”. For the reactive events at the active site, we followed the convention that atoms whose type changes during a reaction are assigned the original type up until the transition state and the product type in the final state. Ethylene and allyl C atoms were modeled with  $sp^2$  C van der Waals parameters through to the transition-state structure and changed to  $sp^3$  parameters in the product. Alkyl carbon and hydrogen atoms of the active site were assigned “CT” and “HC” van der Waals parameters, respectively. Hydride and dihydrogen atoms were assigned the “HC” parameter. Zirconium was represented by the “Zr3+4” van der Waals parameter of Rappé's universal force field (UFF).<sup>22</sup> Electrostatic interactions were not included in the molecular mechanics potential. The justification for this approach has been discussed in previous papers.<sup>8</sup>

**Stationary Points.** All structures labeled **1** through **9** are stationary points on the combined QM/MM potential surface. Structures **2**, **4**, and **8** are transition states; all other structures are minima. Geometry optimizations were terminated if the largest component of the Cartesian gradient was smaller than

(6) Kohn, W.; Sham, L. J. *Phys. Rev. A* **1965**, *140*, 1133.  
 (7) Baerends, E. J.; Ros, P. *Int. J. Quantum Chem. Symp.* **1978**, *12*, 169.  
 (8) Deng, L.; Woo, T. K.; Cavallo, L.; Margl, P.; Ziegler, T. *J. Am. Chem. Soc.* **1997**, *119*, 6177.  
 (9) Baerends, E. J.; Ellis, D. E.; Ros, P. *Chem. Phys.* **1973**, *2*, 41.  
 (10) Snijders, J. G.; Baerends, E. J.; Vernooijs, P. *At. Nucl. Data Tables* **1982**, *26*, 483.  
 (11) Vernooijs, P.; Snijders, J. G.; Baerends, E. J. *Slater Type Basis Functions for the Whole Periodic System*; Department of Theoretical Chemistry, Free University: Amsterdam, The Netherlands, 1981.

(12) Krijn, J.; Baerends, E. J. *Fit Functions in the HFS Method*; Department of Theoretical Chemistry, Free University: Amsterdam, The Netherlands, 1984.

(13) Vosko, S. H.; Wilk, L.; Nusair, M. *Can. J. Phys.* **1980**, *58*, 1200.

(14) Becke, A. *Phys. Rev. A* **1988**, *38*, 3098.

(15) Perdew, J. P. *Phys. Rev. B* **1986**, *33*, 8822–8824.

(16) Perdew, J. P. *Phys. Rev. B* **1986**, *34*, 7406.

(17) Snijders, J. G.; Baerends, E. J. *Mol. Phys.* **1978**, *36*, 1789.

(18) Snijders, J. G.; Baerends, E. J.; Ros, P. *Mol. Phys.* **1979**, *38*, 1909.

(19) Deng, L.; Ziegler, T.; Woo, T. K.; Margl, P.; Fan, L. *Organometallics* **1998**, *17*, 3240.

(20) Cornell, W. D.; Cieplak, P.; Bayly, C. I.; Gould, I. R.; Ferguson, D. M.; Spellmeyer, D. C.; Fox, T.; Caldwell, J. W.; Kollman, P. A. *J. Am. Chem. Soc.* **1995**, *117*, 5179.

(21) Maseras, F.; Morokuma, K. *J. Comput. Chem.* **1995**, *16*, 1170.

(22) Rappé, A. K.; Casewit, C. J.; Colwell, K. S.; Goddard, W. A. I.; Skiff, W. M. *J. Am. Chem. Soc.* **1992**, *114*, 10024.

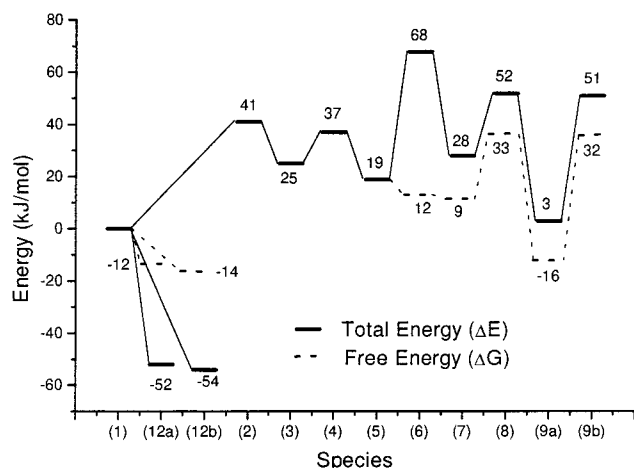


**Figure 1.** Total QM/MM energy (solid) and free energy (dotted; gas phase at 1 bar monomer pressure and 300 K) profile for the formation of the allyl dihydrogen complex (**1** → **5**), elimination of dihydrogen (**6**), and subsequent restart of polymerization (**7** → **9**). For comparison, the ethylene uptake by the agostic precursor (**1** → **12**) is also shown. It was assumed that for unimolecular reaction steps,  $\Delta E = \Delta G$ . For **5**, **6**, and **7**, free energy differences are based on frequency calculations. For **12a** and **12b**, free energies of formation were calculated under the assumption that the ZPE and  $T\Delta S$  contribution to  $\Delta G$  added up to 40 kJ/mol at 300 K and 1 bar.

0.0015 au. Transition states were located in linear-transit fashion. Here, the reaction coordinate (a specific bond length in all calculations) is kept fixed while optimizing all other degrees of freedom. The length of the constrained degree of freedom is varied until the force acting on it is smaller than 0.0015 au. No symmetry constraints were employed. A recent study by Jensen and Børve on Ti ethylene insertion reactions concluded that the BP86 is exceptionally well suited to reproduce high-level ab initio coupled cluster calculations for this type of reactions.<sup>23</sup>

No zero-point energy (ZPE) corrections or thermal corrections were added except for species **5**, **6**, and **7**, for which these corrections are expected to be crucial. ZPE and thermal corrections for **5**, **6**, and **7** are based on harmonic frequency calculations for the generic systems **5'**, **6'**, and **7'**, which we deemed sufficiently similar to the "real" species **5**, **6**, and **7** to warrant transferability. In the frequency calculations, the Cp rings and the ansa-bridge remained frozen to save computer time. We estimate tentative error bars for errors arising from a misrepresentation of the shape of the potential surface by the harmonic approximation.<sup>31</sup> The error bars are  $\pm 10$  kJ/mol for  $T\Delta S_{\text{vib}}$  (at 300 K),  $\pm 5$  kJ/mol for  $\Delta ZPE$ , and  $\pm 2$  kJ/mol for  $\Delta H_{\text{vib}}$  (at 300 K).

## Results and Discussion

We have calculated an energy profile leading from the precursor to insertion (the  $\beta$ -agostic alkyl complex) DPZ-(C<sub>3</sub>H<sub>7</sub>)<sup>+</sup> (**1**) to the product of ethylene insertion into the eventually formed DPZ(C<sub>3</sub>H<sub>5</sub>)<sup>+</sup> complex (**6**), DPZ(hex-5-en-1-yl)<sup>+</sup> (**9**). Figure 1 and Table 1 show the total QM/MM energy of all species involved in this process. Table 2 gives the thermal, entropic, and zero-point corrections for the steps that determine the stability of the DPZ-(C<sub>3</sub>H<sub>5</sub>)<sup>+</sup> complex (**6**). We have also included the energies of formation of the  $\beta$ -agostic frontside and backside  $\pi$ -complexes (**12a** and **b**), as these can act as drains that divert flux away from the  $\beta$ -elimination side reaction.

**Table 1.** Contributions to the Total Energy<sup>d</sup>

	$\Delta E_{\text{QMMM}}^a$	$\Delta E_{\text{MM}}^b$	$\Delta E_{\text{QM}}^c$
<b>1</b>	0	0	
<b>2</b>	41	0	
<b>3</b>	25	-2	
<b>4</b>	37	-3	
<b>5</b>	19	1	17
<b>6</b>	68	-2	67
<b>7</b>	28	6	11
<b>8</b>	52	6	
<b>9a</b>	3	-2	
<b>9b</b>	51	0	
<b>12a</b>	-52	4	
<b>12b</b>	-54	5	

<sup>a</sup> Total energy. <sup>b</sup> MM contribution to the total energy. <sup>c</sup> Difference of the total energies of the generic species (i.e., the one without MM system) and species **1** of the QM/MM system. <sup>d</sup> All values in units of kJ/mol.

### (a) $\beta$ -Hydride Elimination and Allyl Formation.

Formation of an allyl complex from Cp<sub>2</sub>ZrR<sup>+</sup> was first discovered experimentally by Richardson et al.,<sup>4</sup> who during mass spectroscopic investigations found that an allyl group is formed from an alkyl under ejection of a dihydrogen molecule. One can infer from this that the dihydrogen ligand is unstable or only marginally stable under experimental conditions. Indeed, in a previous computational study<sup>3,24</sup> on the "constrained-geometry" catalyst (SiH<sub>2</sub>)Cp(NH)R<sup>+</sup>, we have found that the allyl dihydrogen complex (SiH<sub>2</sub>)Cp(NH)(CH<sub>2</sub>CHCH<sub>2</sub>)(H)<sup>+</sup> is indeed much more stable than the hydrido olefin complex (SiH<sub>2</sub>)Cp(NH)(CH<sub>2</sub>CHCH<sub>3</sub>)(H)<sup>+</sup> in terms of potential energy.

It was, however, not clarified whether such a complex would still be stable on the free energy surface and, hence, under typical experimental conditions. Also, we know of no available experimental data on dihydrogen evolution with the constrained-geometry systems. Some experimental evidence for the formation of dihydrogen under typical polymerization conditions comes from Union Carbide.<sup>5</sup> It was claimed<sup>5</sup> that the DPZ catalyst (Scheme 3) evolves a noticeable amount of dihydrogen in the headspace of slurry ethylene polymerization. It was concluded that this hydrogen is evolved through the allyl formation mechanism investigated here. Our energetic data show that the initial step toward formation of an allyl, namely, the  $\beta$ -hydride elimination, is quite feasible for the DPZ system. An activation barrier of only 41 kJ/mol separates the olefin hydride species **3** from the agostic precursor **1**. In this context it is interesting to note that the total energies of  $\gamma$ - and  $\beta$ -agostic precursors are identical within the resolution of the method (i.e., 1 kJ/mol). Similar energetics have been found previously for the constrained-geometry catalyst CGCTi(propyl)<sup>+</sup>.<sup>3</sup> Also, species **3** is remarkably stable, only 25 kJ/mol above **1**. For comparison, the elimination step for CGCTi(propyl)<sup>+</sup> had an activation barrier of 67 kJ/mol measured from the energetically lowest agostic precursor. Also, the olefin hydride species in that case was 54 kJ/mol above the agostic precursor.

The thermodynamic stability of the elimination product **3** as well as the kinetic facility of the elimination process are caused by a release of steric strain around the active site throughout the elimination process. A

(23) Jensen, V.; Børve, K. *J. Comput. Chem.* **1998**, *19*, 947.

(24) Woo, T. K.; Margl, P.; Ziegler, T.; Blöchl, P. E. *Organometallics* **1997**, *16*, 3454.



**Table 2.** Decomposition of Free Energy Differences (kJ/mol)<sup>a</sup>

	$\Delta G$	$\Delta H$	$\Delta E_{\text{QMMM}}$	$\Delta E_{\text{ZPE}}$	$\Delta pV$	$\Delta H_{\text{tra}}$	$\Delta H_{\text{rot}}$	$\Delta H_{\text{vib}}$	$T\Delta S_{\text{tra}}$	$T\Delta S_{\text{rot}}$	$T\Delta S_{\text{vib}}$
<b>5</b>	7	-37	-49	18	-2	-4	-2	2	-35	-5	-4
<b>6</b>	0	0	0	0	0	0	0	0	0	0	0
<b>7</b>	-3	-47	-40	-8	-2	-4	-4	11	-45	-23	24

<sup>a</sup> Values for **5**, **6**, and **7** are based on frequency calculations on the generic systems **5'**, **6'**, and **7'** (see Computational Details) and are measured relative to the "naked" allyl **6**. Temperature 300 K, pressure 1 bar.

configuration of a loosely bound olefin and a tightly bound, but small, hydride is favored over a tightly bound and sterically bulky alkyl complex.<sup>25</sup> The low barrier is a natural consequence of this, as steric strain is released gradually throughout the process, thus lowering the barrier. A detailed discussion of factors that influence  $\beta$ -elimination energetics and dynamics will be given in a forthcoming paper.<sup>26</sup>

Comparing this to available theoretical data on the insertion barrier of the (Cp)<sub>2</sub>Zr catalyst<sup>27</sup> (17 kJ/mol at the same level of theory as employed here), we can assume that at 300 K elimination events take place fairly frequently compared to insertion events. Assuming an equal population of  $\pi$ -complex (precursor to insertion) and agostic alkyl complex, we would expect one elimination for roughly every 15 000 insertions.

Starting from the olefin hydride, the dihydrogen allyl (**5**) species can be formed via a  $\sigma$ -bond metathesis mechanism with a very small activation barrier of 12 kJ/mol, which is smaller than the barrier leading back to the alkyl precursor (16 kJ/mol). One can therefore safely assume that a  $\beta$ -elimination process will in most cases directly lead to the dihydrogen allyl species (**5**). Very similar behavior was previously found for the CGCTi(propyl)<sup>+</sup> catalyst, which had a barrier of only 3 kJ/mol separating the olefin hydride species from the allyl dihydrogen species.<sup>3</sup> One might therefore assume that the ease with which a dihydrogen allyl complex is formed is a feature common to d<sup>0</sup>, group 4 transition metal catalysts. This conclusion seems even more valid considering the small variation of the molecular mechanics energy term ( $\Delta E_{\text{MM}}$ ), whose magnitude is consistently below 10 kJ/mol for all structures investigated here (Table 1). This is an indicator that the bulky ligand system does not strongly interfere with events at the catalytic site, and therefore the energetics we discuss here should be relatively independent of the steric bulk attached to the Cp ligands. It seems, therefore, that this reaction path is bound to play a role in any polymerization process using this class of catalysts.

#### (b) Chain Propagation from the Allyl Complex.

It was suggested by Resconi<sup>2</sup> that either the allyl dihydrogen species (**5**) or the allyl species **6**—formed after dissociation of dihydrogen from the active site—would be in some way "torpid" with respect to further insertion of olefin and, thus, chain propagation. To further investigate this issue, we calculated the energetics of dihydrogen dissociation from **5** and the reaction steps that would have to follow if the catalyst was to re-enter the propagation cycle at this point.

Figure 1 shows that the dihydrogen dissociation process (**5**  $\rightarrow$  **6**) is energetically quite expensive, with a  $\Delta E_{\text{QMMM}}$  of 49 kJ/mol, without inclusion of ZPE effects. A calculation on the generic systems ( $\Delta E_{\text{QM}}$  (**5'**  $\rightarrow$  **6'**) = 50 kJ/mol) reveals that the contribution of steric bulk to this process is quite small. However, this barrier is quite deceiving, since the entropy change for this bimolecular reaction is very large at an H<sub>2</sub> partial pressure of 1 bar, as is the ZPE correction term, due to the dissociation of a strong metal–H<sub>2</sub> bond. Entropic and ZPE contributions actually turn the reaction **5**  $\rightarrow$  **6** exergonic by 7 kJ/mol. Therefore, dihydrogen ejection from **5** will be spontaneous at elevated temperatures and low H<sub>2</sub> partial pressure. Applying the same corrections to the CGCTi(propyl) system,<sup>3</sup> where the H<sub>2</sub> ejection endothermicity was calculated to be 46 kJ/mol, we again obtain a slightly exergonic reaction ( $\Delta G$  = -5 kJ/mol). Therefore, dihydrogen ejection appears a common feature for group 4, d<sup>0</sup> metal catalysts. The allyl dihydrogen species itself is not "torpid" in the sense that it will significantly retard the propagation process. Instead, it will directly give rise to the allyl complex **6**, whose aptitude toward chain propagation we will investigate next.

To restart chain propagation, the allyl complex **6** has to insert an ethylene monomer. It is a necessary prerequisite for this insertion that the allyl–ethylene complex (**7**) is energetically accessible. In the present case, formation of **7** from **6** has a  $\Delta E_{\text{QMMM}}$  of -40 kJ/mol. ZPE corrections and entropic terms turn the ethylene uptake reaction (**6**  $\rightarrow$  **7**) slightly exergonic by 3 kJ/mol at 1 bar ambient pressure, Table 2.<sup>32</sup> This means that lifetime as well as concentration of **7** will be comparable to the concentration of **6** at 300 K and 1 bar monomer partial pressure. As the ethylene partial pressure is increased, however, the concentration of **7** will be increased relative to the concentration of **6**. Note the contribution of steric bulk to the total energy of reaction **6**  $\rightarrow$  **7** as evidenced by a pure QM calculation in Table 2. The generic bis-Cp system **6'** binds ethylene 17 kJ/mol tighter than the sterically bulkier indenyl system **6**. We expect, therefore, that restarting the chain propagation from a "naked" allyl complex will become increasingly difficult as the size of the catalytic site decreases or monomer size increases.

The ethylene is inserted via a transition state **8**, giving rise to a vinyl-terminated chain (**9**). The transition state is reached through approach of an ethylene carbon atom toward the closest carbon atom of the allyl group. In the transition state, one observes a shift from allylic bonding toward olefinic bonding, in fact much the same as during a  $\sigma$ - $\pi$ -rearrangement. Here the  $\gamma$ -carbon of the new chain becomes sp<sup>3</sup> hybridized, whereas the originally delocalized allylic electron pair forms the olefinic double bond. This transition state (**8**) is 24 kJ/mol higher in energy than the allyl olefin complex (**7**).

(25) Prosenc, M.-H.; Brintzinger, H.-H. *Organometallics* **1997**, *16*, 3889.

(26) Margl, P.; Deng, L.; Ziegler, T. *J. Am. Chem. Soc.*, in press.

(27) Lohrenz, J. C. W.; Woo, T. K.; Ziegler, T. *J. Am. Chem. Soc.* **1995**, *117*, 12793.

This is not high enough to render the allyl **6** inactive. However, the insertion product (**9a**) might be inert with respect to further propagation, as it contains a  $\pi$ -complexed vinyl terminus. This coordinative saturation of the metal center might prevent further complexation of monomer and, thus, chain propagation.

For the DPZ catalyst, the insertion product (**9**) lies only 16 kJ/mol below the agostic precursor (**1**) in terms of free energy (Figure 1). We will here assume that further insertion into the M–R bond would take place by (a) dissociation of the  $\pi$ -complexed terminal vinyl group from the metal center, leaving the metal center with only an alkyl bond. In a second step (b), an incoming olefin would attach itself to the active site and insert into the M–hexenyl  $\sigma$ -bond. We have calculated the energy required to perform step a of this process as amounting to 48 kJ/mol. We did this by straightening the 1-hexenyl chain such that the vinyl terminus was dissociated from the metal center, while the remainder of the chain was allowed to assume a low-energy configuration in a local  $\beta$ -agostic minimum **9b**. After completion of step a, the metal center is left once again unsaturated, as in the agostic precursor **1**. We can now use our previous results for the complexation of ethylene to the coordinatively unsaturated,  $\beta$ -agostic precursor **1** (–52 to –54 kJ/mol) to extrapolate the energy gain of step b (complexation of ethylene to **9a**) as –4 to –6 kJ/mol. In case steps a and b happen asynchronously, one would have to reckon with a substantial buildup of **9**, since the barrier for dissociation of the  $\pi$ -complexed vinyl terminus is rather high (48 kJ/mol). However, this process can also happen synchronously, with the incoming ethylene dislodging the vinyl chain end from the metal. In the latter case, previous experience with second-order substitutions of  $\pi$ -complexed olefin with  $\pi$ -complexed olefin states that there will be no appreciable energy barrier, but a considerable free energy barrier due to a large (unfavorable) entropic contribution to the displacement of the vinyl terminus by ethylene, arising from the chelate effect. Our calculations for the reaction **6**  $\rightarrow$  **7** as well as experimental evidence and previous calculations on the same type of reaction show that there is about 40–50 kJ/mol positive entropic contribution to this process at 1 bar partial pressure and 300 K.<sup>33</sup> This acts as an effective barrier toward displacement of the vinyl terminus. However, typical technological processes do not run at such low monomer pressure. For processes run under high monomer pressure, we assume the displacement process to be thermoneutral and barrierless. This allows the conclusion that the insertion product of allyl and ethylene (**9**) will be sufficiently reactive to restart chain propagation. Only under extremely low monomer partial pressure would there be a buildup of compound **9** in the reactor.

We expect the restart of chain propagation to be much more difficult if higher  $\alpha$ -olefins are used as monomers. The complexation of ethylene to  $d^0$  transition metal centers is dominantly influenced by the sterics around the metal center.<sup>28</sup> If the metal center becomes more congested, the entrance channel for the olefin becomes constricted and complexation quickly becomes impossible. For more sterically encumbered metallocenes or

metallocenes with small metal ions (e.g., titanocene), ethylene complexation is actually endergonic.<sup>28</sup> This can be expected to hold true also for sterically more demanding monomers, such as propene.  $\alpha$ -Olefins higher than ethylene will experience more difficulty in restarting chain propagation than ethylene. This means that there is a longer lifetime for the “naked” allyl **6** and, thus, a higher danger of allyl buildup and eventual catalyst deactivation. Karol's group<sup>5</sup> also observed the number of internal unsaturations dwindle as the  $H_2$  partial pressure was increased. Resconi<sup>2</sup> also observed that applying dihydrogen under pressure can “revive” a deactivated catalyst, which is in agreement with our calculations.

We conclude that, for the DPZ catalyst system and ethylene monomer, the allyl mechanism will not lead to catalyst deactivation. For higher  $\alpha$ -olefins and sterically more constricted catalysts, however, we expect a lowering of the activity of the catalyst due to longer dormancy time at the allyl stage.

### Conclusions

We have shown by theoretical calculations on the DPZ catalyst system that (a)  $\beta$ -hydride elimination from the growing chain is a kinetically as well as thermodynamically feasible process that is likely to occur for most metallocene type, group 4,  $d^0$  catalysts. The kinetic and thermodynamic feasibility of this process is driven by the release of steric energy that accompanies the formation of the olefin hydride complex. (b) The formation of a dihydrogen allyl complex from the olefin hydride is a kinetically fast as well as thermodynamically favorable process. We expect that a significant fraction of  $\beta$ -hydrogen eliminations will lead to the allyl dihydrogen product. Based on comparisons with previous theoretical results on the constrained-geometry catalyst, we speculate that this is a feature common to metallocene type catalysts in general. (c) Release of dihydrogen from this allyl dihydrogen complex is spontaneous at 1 bar dihydrogen pressure and 300 K and driven by a loss of zero-point energy and gain of translational entropy. As dihydrogen is released, a “naked” allyl complex is formed. (d) Restart of chain propagation is feasible for the combination of ethylene monomer and DPZ catalyst, as the ethylene monomer is small enough to bind to the metal that is shielded by the tightly bound allyl. The insertion barrier for ethylene into the metal–allyl bond is 24 kJ/mol, which is small enough to allow restart of the chain without substantial delay. For smaller metal ions and/or geometrically more constricted Cp ligand systems, we expect considerable difficulties in restarting the chain, since the metal site becomes too constricted

(29) Rix, F. C.; Brookhart, M.; White, P. S. *J. Am. Chem. Soc.* **1996**, *118*, 4746.

(30) Musaev, D. G.; Froese, R. D. J.; Svensson, M.; Morokuma, K. *J. Am. Chem. Soc.* **1997**, *119*, 367.

(31) There is a crucial issue involved in calculating thermodynamic properties from a harmonic force field: the vibrational entropy computed from harmonic frequencies is extremely error-prone since the harmonic approximation is rather inadequate for low-frequency modes. In the present cases (**5'**, **6'**, **7'**), the loosely bonded active site exhibits between 7 (**5'** and **6'**) and 12 (**7'**) frequencies in the sensitive range below 300  $cm^{-1}$ . It is recommended practice to replace the harmonic approximation for these low-lying modes with a more realistic expansion of the potential surface. However, in the present case this is extremely difficult, since none of the modes involved can be described within one of the well-known approximations such as the hindered-rotor model.

(28) Margl, P.; Deng, L.; Ziegler, T. *Organometallics* **1998**, *17*, 933.

to allow entrance of the monomer. This would result in lower chain lengths and eventual catalyst deactivation. (e) Applying dihydrogen under pressure, thus shifting the olefin-hydride/dihydrogen-allyl equilibrium to the left, can revive the "torpid" allyl complex. This result is also experimentally borne out.<sup>2</sup> (f) The internal unsaturation created by the allyl mechanism binds in a  $\pi$ -complex fashion to the active site. This poses some danger of decreasing the activity of the catalyst, as the internal olefin tightly occupies the coordination site reserved for the incoming monomer through the chelate effect. With an activation barrier of 48 kJ/mol, removal of the internal  $\pi$ -complex is the energetically most costly step in the profile investigated here. However, this will not be a problem at high monomer partial pressure.

---

(32) Note that the ZPE and vibrational entropy contributions to the ethylene capture reaction (**6**  $\rightarrow$  **7**) are somewhat counterintuitive. A closer inspection of vibrational frequencies of **7** reveals that the metal-ligand framework of **7** is substantially weakened by the intrusion of a new ligand. This increases the number of vibrational frequencies below 400 cm<sup>-1</sup> by **7**, leading to a low zero-point energy of **7** and a rather large stabilization by vibrational entropy. See also the Computational Details section for a discussion of the accuracy of vibrational contributions to the free energy.

**Acknowledgment.** This investigation has been supported by the National Sciences and Engineering Research Council of Canada (NSERC) and by the donors of the Petroleum Research Fund, administered by the American Chemical Society (ACS-PRF No. 31205-AC3), as well by Novacor Research and Technology Corporation (NRTC) of Calgary. The Izaak Walton Killam Memorial Foundation is highly appreciated by T.Z. (Canada Council Killam Professor) and T.K.W. (Killam graduate fellowship). T.K.W. also thanks NSERC and the Alberta Heritage Scholarship for graduate fellowships, and Dr. E. Wasserman for providing a preprint of his work. P.M. would like to thank Dr. Luigi Resconi (Montell Italia) for many fruitful discussions and for providing a preprint of his work.

**Supporting Information Available:** A listing of Cartesian coordinates and a full listing of the molecular mechanics parameters (9 pages). Ordering information is given on any current masthead page.

OM980424Q

---

(33) Although there is little experimental data available, existing evidence suggests that the  $-T\Delta S$  contribution to the free energy of ethylene complexation for early transition metal d<sup>0</sup> compounds is identical to the 40–50 kJ/mol one observed at 300 K for late transition metal (Ni and Pd) d<sup>8</sup> compounds.<sup>29,30</sup>